

Thin Film Transistor Gas Sensors Incorporating High-Mobility Diketopyrrolopyrrole-Based Polymeric Semiconductor Doped with Graphene Oxide

Kwang Hee Cheon,[†] Jangwhan Cho,[†] Yun-Hi Kim,^{*,‡} and Dae Sung Chung^{*,†}

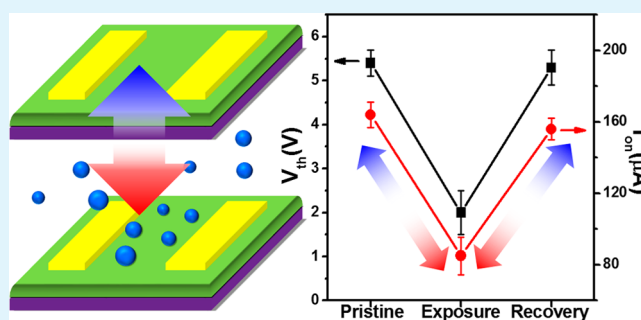
[†]School of Chemical Engineering and Material Science, Chung-Ang University, Seoul 156-756, Korea

[‡]Department of Chemistry and ERI, Gyeongsang National University, Jinju 660-701, Korea

Supporting Information

ABSTRACT: In this work, we fabricated a diketopyrrolopyrrole-based donor–acceptor copolymer composite film. This is a high-mobility semiconductor component with a functionalized-graphene-oxide (GO) gas-adsorbing dopant, used as an active layer in gas-sensing organic-field-effect transistor (OFET) devices. The GO content of the composite film was carefully controlled so that the crystalline orientation of the semiconducting polymer could be conserved, without compromising its gas-adsorbing ability. The resulting optimized device exhibited high mobility ($>1 \text{ cm}^2 \text{ V}^{-1} \text{ s}^{-1}$) and revealed sensitive response during programmed exposure to various polar organic molecules (i.e., ethanol, acetone, and acetonitrile). This can be attributed to the high mobility of polymeric semiconductors, and also to their high surface-to-volume ratio of GO. The operating mechanism of the gas sensing GO-OFET is fully discussed in conjunction with charge-carrier trap theory. It was found that each transistor parameter (e.g., mobility, threshold voltage), responds independently to each gas molecule, which enables high selectivity of GO-OFETs for various gases. Furthermore, we also demonstrated practical GO-OFET devices that operated at low voltage ($<1.5 \text{ V}$), and which successfully responded to gas exposure.

KEYWORDS: gas sensor, high sensitivity, gas detector, graphene oxide, organic field effect transistor



INTRODUCTION

Graphene has attracted great attention as an active layer in gas sensors due to its outstanding electrical properties and high surface-to-volume ratio.¹ Researchers have reported that graphene can detect even the lowest concentrations of gas species, and that the dynamic range of detection may cover the range from a single molecule to very high concentrations.² Here one needs to note that pristine graphene does not have dangling bonds on its surface, which are essential for detecting gas molecules. This means that in most cases, functionalized graphene has been used for gas-sensing applications because of the presence of suitable hydrophilic groups on its surface.³

To achieve high-sensitivity graphene-based gas sensor, various device geometries have been designed, including resistive sensors,⁴ transistor sensors,⁵ surface acoustic wave sensors,⁶ quartz crystal microbalance sensors,⁷ and microelectromechanical systems.⁸ Among these, transistor-based gas sensors have been most widely studied due to a greater sensing ability enabled by gate-tunable current modulation. In addition, transistors constructed based on organic materials could lead to high-end applications such as lightweight, flexible, wearable devices. Therefore, combining the gas-adsorbing ability of graphene oxide (GO) and the current modulating ability of organic field effect transistors (OFETs) has been the goal of

recent research in the field of gas-sensing research.^{9–12} The sensing mechanism of such GO-OFET gas sensors is as follows. During adsorption of polar gas molecules by graphene oxide, which has a physical interface with the polymeric semiconductor, hole charge carriers in the semiconductor layer come across additional trapping centers, which leads to the change of mobile charge carrier densities in the channel region of OFETs. This phenomenon may induce changes in various OFET parameters, including threshold voltage, charge carrier mobility, subthreshold swing, and on/off ratio.¹¹

For example, Y. Kim and co-workers introduced modified graphene oxide/poly(9,9'-dioctyl-fluorene-co-bithiophene: F8T2)-blend films for acetone and ethanol detection in the form of OFETs.¹¹ In other work, T. Xie and co-workers applied reduced graphene oxide/poly(3-hexylthiophene: P3HT)-bilayer films for detection of nitrogen dioxide, also in the form of OFETs.¹² In both studies, the authors analyzed the shift of threshold voltage and charge carrier mobility of OFETs, in relation to gas exposure. These previous works contributed a lot to the field in terms of utilizing commercially available and

Received: April 8, 2015

Accepted: June 12, 2015

Published: June 12, 2015

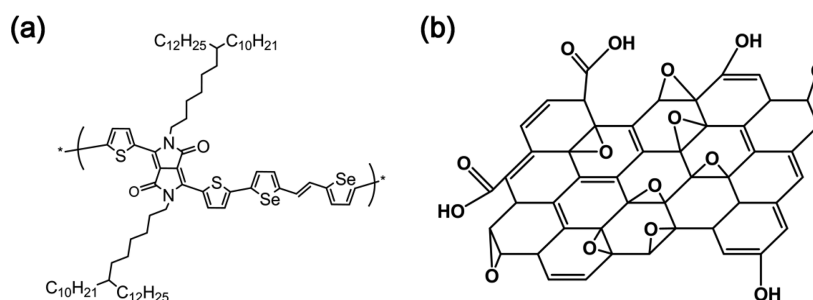


Figure 1. Chemical structure of (a) DPP-SVS and (b) functionalized graphene oxide used in this work.

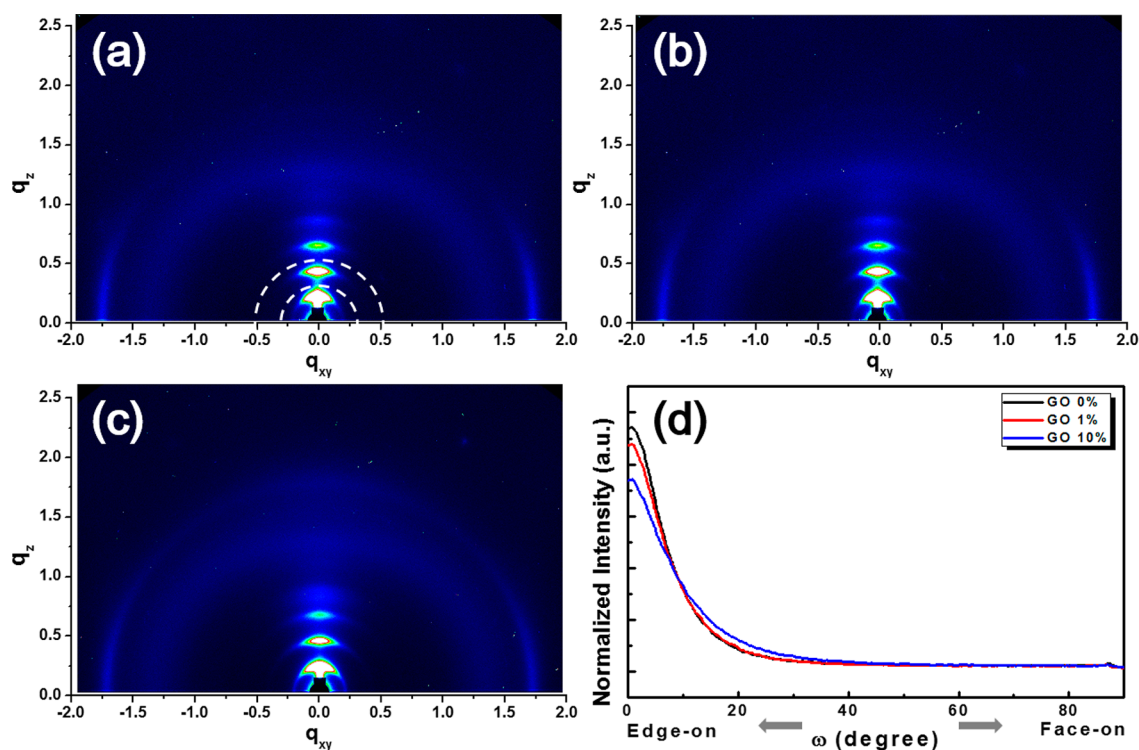


Figure 2. GIXD images of composite films with GO contents of (a) 0, (b) 1, and (c) 10%. (d) shows pole figure analysis results.

representative polymeric semiconductors to create a GO-OFET gas sensor. However, the work was fundamentally limited by the low mobility of the polymeric semiconductors they used. Both P3HT and F8T2 have charge carrier mobilities on the order of $10^{-2} \text{ cm}^2 \text{ V}^{-1} \text{ s}^{-1}$, which is much lower than that of inorganic semiconductors.¹³ The transit time within a semiconductor sandwiched between two electrodes can be determined using the following equation, in the case of hopping transport.¹⁴

$$t = \frac{L^2}{V\mu}$$

where L is the channel distance, V is the applied voltage, and μ is the charge carrier mobility. Therefore, one can see that if the mobility is enhanced 1×10^3 times, then the transit time is shortened by the same factor. This means that increasing charge carrier mobility in GO-OFET devices is very important for enhanced gas-sensing ability, especially for rapid sensing.

Recently, donor–acceptor-based copolymers have attracted great attention in the study of OFET due to their unprecedentedly high charge carrier mobility.^{15–18} This originates from enhanced intramolecular charge transport via

strong donor–acceptor charge delocalization. The peak mobility value now exceeds $10 \text{ cm}^2 \text{ V}^{-1} \text{ s}^{-1}$, which is compatible with a realistic minimum requirement for driving FETs of commercial, organic light-emitting diodes.¹⁹ Therefore, we can think about combining these brand-new, high-mobility polymers for GO-OFET applications, to use for their high-quality gas-sensing ability.

For this purpose, we herein introduced a high mobility copolymer, DPP-selenophene-vinylene-selenophene (DPP-SVS),¹⁵ doped with functional graphene oxide as an active layer of the GO-OFET. Owing to both the high adsorbing ability of GO, and the high charge carrier mobility of the DPP-SVS, we were able to demonstrate sensitive detection by the GO-OFET of various gaseous polar organic solvents, including ethanol, acetone, and acetonitrile. The detailed gas-sensing mechanism is fully discussed in relation to charge-carrier trap theory, which explains the possible selectivity of GO-OFETs to specific gas molecules. For practical purposes, we further demonstrated a low voltage operating GO-OFET useful for gas sensing.

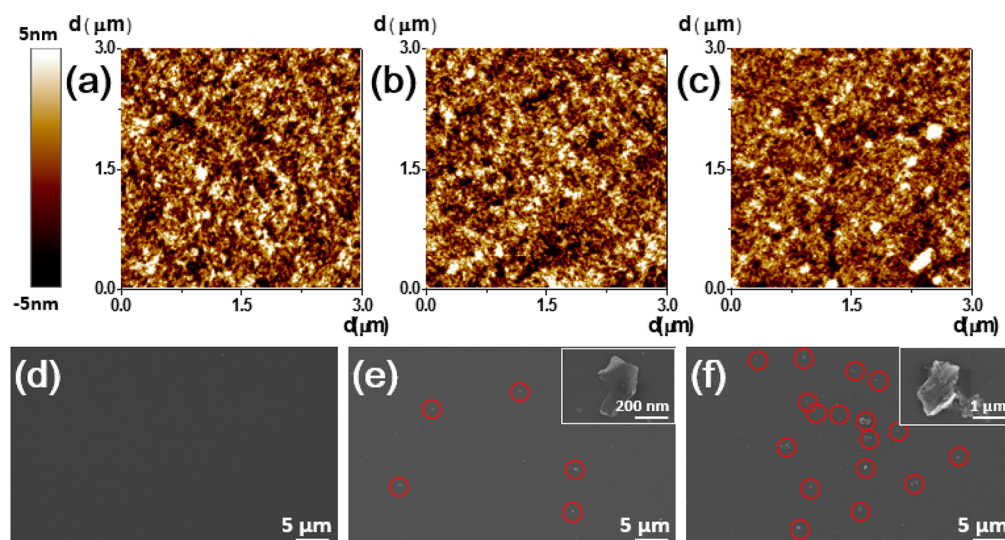


Figure 3. (a–c) AFM images of composite films with GO contents of (a) 0, (b) 1, and (c) 10%. The r.m.s roughness values are 1.12, 1.2, and 1.45 nm for a, b, and c, respectively. (d–f) SEM images of composite films with GO contents of (d) 0, (e) 1, and (f) 10%. Inset shows the enlarged GO images.

EXPERIMENTAL SECTION

Materials. All chemical reagents were purchased from Aldrich and used as received. And GO was purchased from Graphene Supermarket. The flake size was 0.5–5 μm and the solution concentration was 5g/L. The other materials were common commercial level and used as received. All solvents used were further purified prior to use.

Device Fabrication. Top-contact OFETs were fabricated on a common gate of highly n-doped silicon with a 100 nm thick thermally grown SiO_2 dielectric layer. The dielectric layer was further modified by octyltrichlorosilane (OTS) by dipping in toluene solution. Solutions containing the composite were spin-coated at 2000 rpm from 0.5–1 wt % solutions to form thin films with a nominal thickness of 30 nm, as confirmed using a surface profiler (Alpha Step 500, Tencor). The films were not further thermally treated. Gold source and drain electrodes were evaporated on top of the semiconductor layers (80 nm). For all measurements, typical channel widths (W) and lengths (L) were 1000 and 100 μm , respectively.

Measurement. The electrical characteristics of the transistors were measured by 4156A precision semiconductor parameter analyzers (Agilent Technologies) in conjunction with Keithley 2400 source meter. Gas exposure was conducted in closed chamber with vacuum and gas inlet/outlet valve controlled by home-built lab-view program. SEM image was obtained by FE-SEM (Sigma/Carl Zeiss) with Schottky Field Emitter.

Characterization. GIXD data were measured at 3C and 6D beamline of Pohang accelerator laboratory. AFM images were obtained by using an atomic force microscope (AFM: XE-100, PISA).

RESULTS AND DISCUSSION

Figure 1a shows the chemical structure of the semiconducting polymer, DPP-SVS, used as a polymeric semiconductor in this work. Because the thiophene unit is attached to the DPP unit, it is expected that close (2.1 \AA) intramolecular hydrogen bonding would be formed between the carbonyl oxygen of DPP and the nearest thiophene hydrogen, facilitating backbone planarity.²⁰ Consequently, and different from traditional polythiophene-based semiconducting polymers, one could expect much more efficient intermolecular charge transport, and thereby high charge-carrier mobility, once a well-aligned edge-on intermolecular structure is formed. The chemical structure of the functionalized GO used in this work, is shown in Figure 1b.²¹ In contrast to DPP-SVS, GO has many polar functional groups

that can work as sensitizing centers for external polar gaseous organic molecules. Especially, because all the functional groups on GO are directly exposed to the external environment due to the high surface-to-volume ratio of graphene, one could expect very efficient adsorption efficiency of gaseous molecules, even with only a small amount of GO in the composite. The experimental condition of maintaining a small amount of GO in the composite was quite important because the crystalline orientation of polymeric semiconductors can be easily influenced by impurity, mostly leading to a broadened crystalline orientation.

Therefore, finding the minimum amount of GO in the composite film that is still functional for gas sensing is the first priority in this work. In Figure 2, the crystalline orientation of polymer-GO composite films with various GO content, were analyzed by means of 2D grazing incident X-ray diffraction (GIXD) tools. In the 2-D GIXD patterns (Figure 2a–c), q_{xy} and q_z represent the in-plane and out-of-plane components of the scattering vector q , respectively. These components are normal to the plane of incidence and the sample surface plane, respectively. Regardless of the GO content, the 2D GIXD patterns of all the composite films exhibited out-of-plane ($n00$) diffraction peaks, up to fifth-order diffraction. The (100) layer distance, the d -spacing ($= 2\pi/q^*$) derived from the out-of-plane profiles was 26.5 \AA . Additionally, a relative weak peak at $q_{xy} \approx 1.74 \text{\AA}^{-1}$ was observed in the in-plane profiles, which could be attributed to the formation of intermolecular π - π stacking with distance $\sim 3.6 \text{\AA}$. At the same time, one can see the diffraction peaks apparently broaden with increasing GO content. To study further the effect of processing solvents on the crystalline orientation of DPP-TT films, we conducted pole figure analyses (presented in Figure 2d). Pole figure analyses enable the study of the orientational distribution of the diffraction peaks as a function of all possible crystalline orientations.²² To construct the pole figure, we analyzed the distribution of (200) orientations to avoid the surface scattering effects resulting from the substrate. This analysis showed that the relative pole figure intensity near a polar angle 0° increased as in the sequence of GO content in the composite: 10% < 1% < 0%, implying that in this sequence, preferential edge-on structure

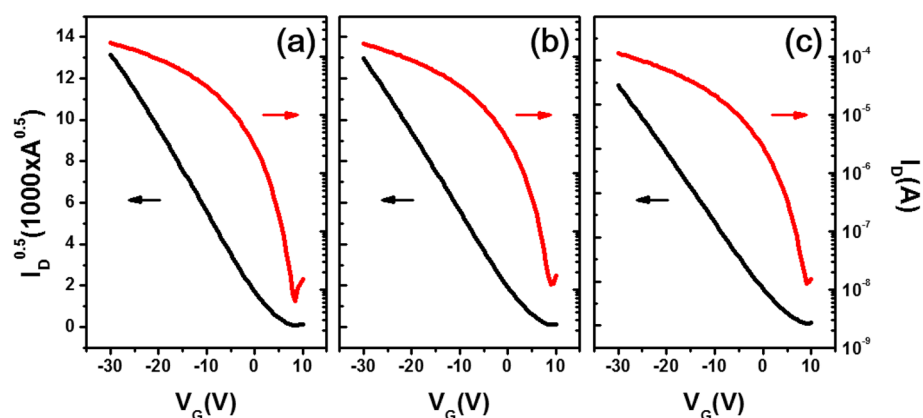


Figure 4. Saturation transfer characteristics of OFETs based on composite films with GO contents of (a) 0, (b) 1, and (c) 10%.

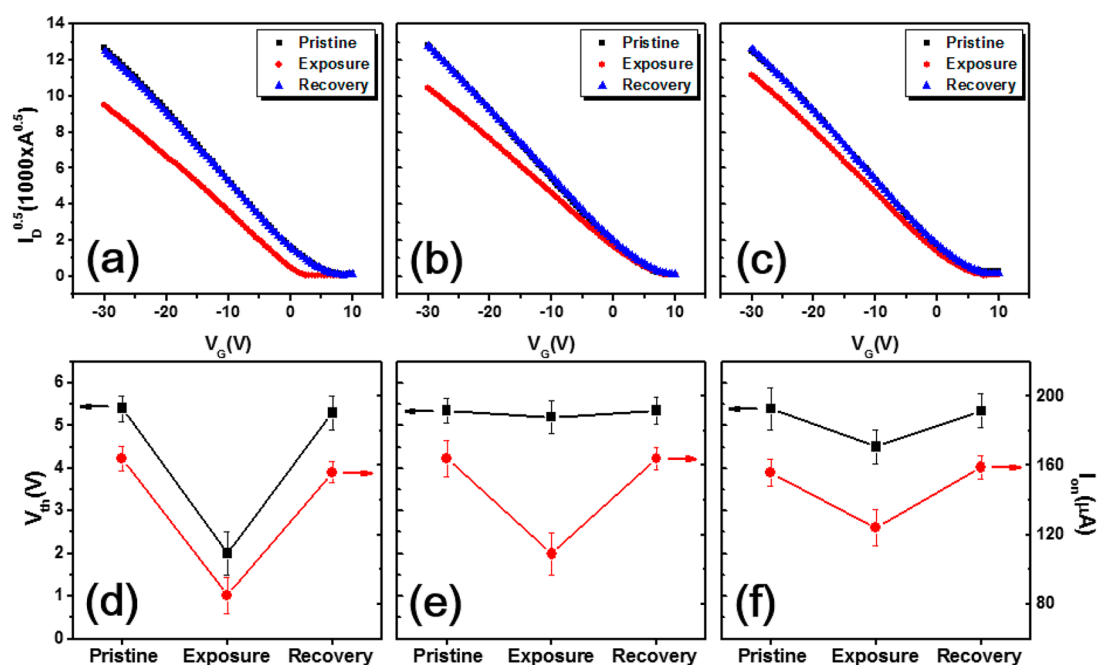


Figure 5. Transistor behaviors under the programmed gas exposure. Upper panel corresponds to transfer curves and lower panel corresponds to the summary on the shift of V_{th} and on-current (or the slope) values. (a, d) Ethanol, (b, e) acetone, (c, f) acetonitrile. (To construct error ranges, we analyzed 30 independent GO-OFETs.)

was more developed. Therefore, we decided to fabricate GO-OFET devices for gas sensing with composite consisting of 1% GO and 99% polymeric semiconductor, to minimize structural loss.

Figure 3a–c shows images of the surface topography of the above-mentioned three composite films with different GO content. In a similar context with GLXD analyses, we could observe sequential increase of r.m.s. roughness as a result of increasing content of GO in the composite. From Figure 3 (d–f), we could see gradual increase of surface density of GO in the composite films as the GO content increases. In the case of 10% GO loading ratio, even micrometer-sized clusters of GO were also observed. The formation of smooth morphology with minimal peak-to-valley deviation is essential to achieve efficient intermolecular charge transport and therefore we concluded that the composite film with 1% GO would be the appropriate condition for device fabrication, if it still shows reasonable gas-adsorbing ability. Actually, as summarized in Figure 4, the field effect mobility of OFET based on composite with 0% GO

showed the highest mobility ($1.2 \text{ cm}^2 \text{ V}^{-1} \text{ s}^{-1}$), while rather low mobilities (1.1 and $0.6 \text{ cm}^2 \text{ V}^{-1} \text{ s}^{-1}$) were observed in the case of 1% GO and 10% GO, respectively. This result can be attributed the loss of edge-on orientation of composite film when doped with more amount of GO.

The gas-sensing ability of the GO-OFETs was tested by measuring transistor characteristics under programmed gas exposure. For all the devices used in this work, we did not use thermal annealing processes: under the thermal annealing, the on-current was slightly enhanced but with decrease in on–off current ratio, resulting in relatively poor sensing ability (Figure S1, Supporting Information). The transfer characteristics of OFETs consisting of only polymeric semiconductor (with 0% GO) revealed negligible changes after ethanol exposure, presumably due to the hydrophobic nature of polymers. In the case of GO-OFETs with 1 and 10% GO, transfer characteristics showed quite similar shifts after ethanol exposure (Figure S2, Supporting Information); therefore, we focused on GO-OFETs with 1% GO, only considering its apparently

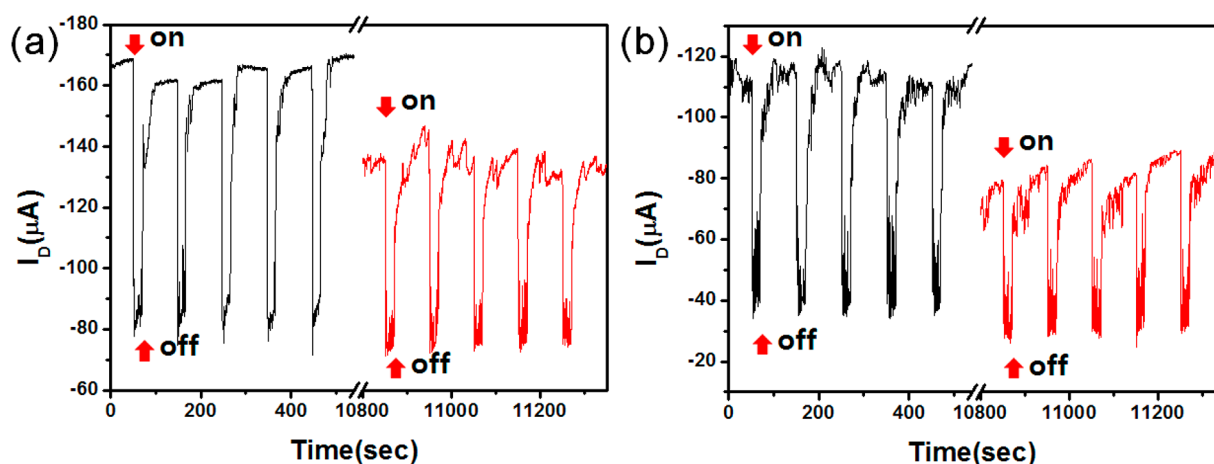


Figure 6. Transient responses of GO-OFETs under programmed ethanol exposure with (a) 1% GO content and (b) 10% GO content. The “gas-on” state was maintained for 20 s and “gas-off” state was maintained for 80 s. The total measurement time was 3 h.

higher charge carrier mobility. This result also means that 1% of GO is enough to adsorb enough gaseous ethanol molecules to change the mobile charge carrier density in the transistor channel area.

Figure 5 shows the transfer behavior of GO-OFETs after exposure to ethanol, acetone, and acetonitrile. The transistor parameters for all the devices under programmed gas exposure are also summarized in Figure 5. The polarity index of these three polar solvents are very similar:²³ 5.2, 5.1, and 5.8 for ethanol, acetone, and acetonitrile, respectively. Accordingly, the exposure of these molecules to GO-OFETs resulted in similar aspects of shift in transfer behavior: the p-type transfer curves shifted to the negative direction and the value of on-current (or the slope) decreased, upon gas exposure. The negative shift of threshold voltage (V_{th}) can be related to increases in the concentration of the deep trap states.²⁴ This means that the polar gaseous molecules adsorbed by GO acted as deep trap states for hole charge carriers because of their polarity. Especially, we could see that the ethanol exposure resulted in a much more pronounced shift of V_{th} of the GO-OFETs, compared to exposure to other solvents. This phenomenon implies that different solvent molecules have different degrees of intermolecular interaction with GO. In other words, the analyses on the V_{th} shifts can be interpreted in this way: a hydroxyl group exists only in ethanol, among the solvents used, and therefore, ethanol molecules may have a higher probability of forming strong hydrogen bonding with the polar groups of GO, leading to a most significant shift in V_{th} . In contrast, the decrease of on-current (or the slope) of transfer curve by gas exposure, which could be directly related to the decreased charge carrier mobility, is thought to originate from the increased shallow trap density.²⁵ In the presence of shallow trap states, the hole can easily be trapped and the trapped hole can also easily be detrapped in the channel region. Therefore, hole transport is more easily interrupted by multiple trap-and-release behavior. In this case, different from the case of the V_{th} shift, exposure to all the gaseous molecules resulted in similar decrease in mobility. This means that the nature of weak intermolecular interactions between gaseous molecule and GO are very similar regardless of the kind of solvent molecules. Interestingly, after purging the measurement chamber, the transfer curves rapidly recovered to the pristine state, implying that both deep trap and shallow trap states were eliminated by desorption of all the gas molecules. The reproducible shifts of

transfer curves upon programmed gas exposure/inert gas purging are very encouraging, considering the future application of high-mobility GO-OFETs for gas sensing.

The transient responses of GO-OFETs were studied to further demonstrate the fast response of the devices upon gas exposure. In-situ responses of the fabricated GO-OFETs with both 1% and 10% dopant ratios under ethanol exposure were recorded as a function of time. The in situ experiments were programmed as follows: 20 s of exposure and subsequent 80 s of nonexposure, with total program time of 3 h. As summarized in Figure 6 (a) and (b), both GO-OFETs with 1% and 10% GO contents showed prompt responses against ethanol exposure. Upon gas exposure, (gas-on) the I_D rapidly decreased by almost 50% within 1 s, revealing the prompt response-ability of GO-OFET. Furthermore, one can also observe sharp recovering ability of GO-OFET after stopping gas exposure (gas-off): 1 s for 70% recovery and 10 s for 90% recovery. When comparing GO-OFETs with 1% GO and 10% GO content, one can see the overall ascendancy of GO-OFET with 1% GO in terms of signal-to-noise ratio. This result can be attributed to better transistor performance of GO-OFET with 1% GO, enabled by more optimized structure/morphology. The durabilities of GO-OFETs under repeated gas exposure were also tested as highlighted in the right corner of Figure 6. After 3 h of gas exposure test, the GO-OFETs still maintained gas-sensing ability but with slightly decreased current level, presumably due to the oxidation of polymeric semiconductor. Such aging effect was more pronounced in the case of GO-OFET with 10% GO content, which can be attributed to more numbers of functional groups in the composite film. Overall, the fabricated GO-OFETs showed satisfactory transient responses under programmed gas exposure and more importantly, they retained such prompt response-ability even after 3 h of continuous experiments.

Including our own work described above, all the work related to gas-sensing OFETs have been performed at relatively high voltage (>30 V). The operating voltage required to achieve gas-sensing ability from OFETs is still too high in comparison with their inorganic counterparts (e.g., a-Si:H). In addition, considering practical applications of gas sensors, such as for portable devices operated by battery, we definitely need to decrease the operating voltage. Therefore, we tried to fabricate low-voltage GO-OFET devices by replacing the conventional SiO_2 layer with a sol-gel processed ZrO_x layer. By adjusting the

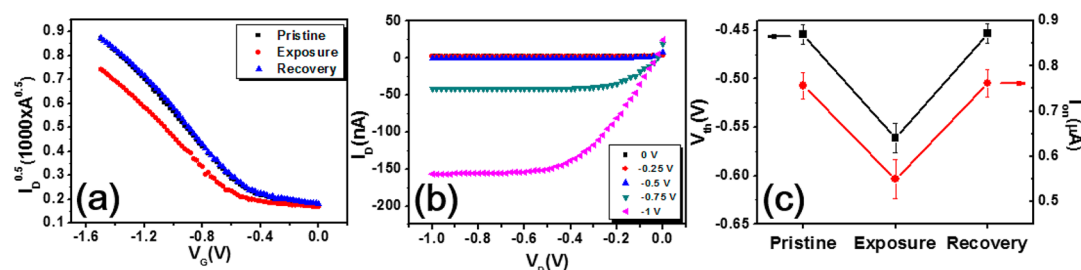


Figure 7. (a) Transfer and (b) output curves of ZrO_x -based low-voltage OFET. (c) Summary of gas exposure behavior. (To construct error ranges, we analyzed 30 independent GO-OFETs.)

thickness of the ZrO_x layer, we could operate GO-OFET within 1.5 V, as shown in Figure 7. Similar to the case of SiO_2 -based devices, the transfer curves showed reproducible response after ethanol exposure. According to the best of our knowledge, this is the first demonstration of a low-voltage GO-OFET.

CONCLUSION

We fabricated a GO-OFET, in which a composite consisting of GO and high-mobility polymeric semiconductors (DPP-SVS), was used as an active layer, for the purpose of gas sensing applications. The optimal content of GO in the composite was determined to be 1% (w/w) to maximize intermolecular interactions of DPP-SVS (and thus charge carrier mobility), without compromising its gas-adsorbing ability. Compared to OFETs with only pristine DPP-SVS, GO-OFETs revealed significantly enhanced gas-sensing ability by showing negative shift of V_{th} as well as decreased on-current (or the slope). The V_{th} shift, which is related to the increased density of the deep trap states, was more pronounced in the case of ethanol exposure. The degree of mobility decrease, which is related to the shallow trap density, was similar regardless of the gas molecules to which the GO-OFET was exposed. The different responses of transistor parameters for different gas molecules, enables high selectivity of GO-OFETs devices. Finally, we demonstrated a low-voltage operated GO-OFETs (within 1.5 V) by fabricating a ZrO_x -based transistor geometry, which also showed a successful responses to gas exposure.

ASSOCIATED CONTENT

Supporting Information

Transfer curves of annealed film with GO 1% content under the ethanol exposure. Transfer curves of composite film with GO content of 10% under the ethanol exposure. The Supporting Information is available free of charge on the ACS Publications website at DOI: 10.1021/acsami.5b03059.

AUTHOR INFORMATION

Corresponding Authors

*E-mail: ykim@gnu.ac.kr.

*E-mail: dchung@cau.ac.kr.

Notes

The authors declare no competing financial interest.

ACKNOWLEDGMENTS

This research was supported by Space Core Technology Development Program through the National Research Foundation of Korea (NRF) funded by the Ministry of Education (Grants NRF-2014M1A3A3A02034707).

ABBREVIATIONS

GO, grapheme-oxide

OFETs, organic field-effect transistors

DPP, diketopyrrolopyrrole

GIXD, grazing-incidence X-ray diffraction

REFERENCES

- Castro Neto, A. H.; Guinea, F.; Peres, N. M. R.; Novoselov, K. S.; Geim, A. K. The Electronic Properties of Graphene. *Rev. Mod. Phys.* **2009**, *81*, 109.
- Basu, S.; Bhattacharyya, P. Recent Developments on Graphene and Graphene Oxide based Solid State Gas Sensors. *Sens. Actuators, B* **2012**, *173*, 1–21.
- Dan, Y.; Lu, Y.; Kybert, N. J.; Luo, Z.; Charlie Johnson, A. T. Intrinsic Response of Graphene Vapor Sensors. *Nano Lett.* **2009**, *9*, 1472–1475.
- Wehling, T. O.; Novoselov, K. S.; Morozov, S. V.; Vdovin, E. E.; Katsnelson, M. I.; Geim, A. K.; Lichtenstein, A. I. Molecular Doping of Graphene. *Nano Lett.* **2007**, *8*, 173–177.
- Leenaerts, O.; Partoens, B.; Peeters, F. M. Adsorption of H_2O , NH_3 , CO , NO_2 , and NO on Graphene: A first-principles Study. *Phys. Rev. B* **2008**, *77*, 125416.
- Arash, B.; Wang, Q.; Duan, W. H. Detection of Gas Atoms via Vibration of Graphenes. *Phys. Lett. A* **2011**, *375*, 2411–2415.
- Yao, Y.; Chen, X.; Guo, H.; Wu, Z. Graphene Oxide Thin Film Coated Quartz Crystal Microbalance for Humidity Detection. *Appl. Surf. Sci.* **2011**, *257*, 7778–7782.
- Pradhan, S. C. Buckling of Single Layer Graphene Sheet Based on Nonlocal Elasticity and Higher Order Shear Deformation Theory. *Phys. Lett. A* **2009**, *373*, 4182.
- Lu, G.; Ocola, L. E.; Chen, J. Gas Detection using Low-temperature Reduced Graphene Oxide Sheets. *Appl. Phys. Lett.* **2009**, *94*, 083111.
- Deng, S.; Tjoa, V.; Fan, H. M.; Tan, H. R.; Sayle, D. C.; Olivo, M.; Mhaisalkar, S.; Wei, J.; Sow, C. H. Reduced Graphene Oxide Conjugated Cu_2O Nanowire Mesocrystals for High-Performance NO_2 Gas Sensor. *J. Am. Chem. Soc.* **2012**, *134*, 4905–4917.
- Kim, Y.; An, T. K.; Kim, J.; Hwang, J.; Park, S.; Nam, S.; Cha, H.; Park, W. J.; Baik, J. M.; Park, C. E. A Composite of a Graphene Oxide Derivative as a Novel Sensing Layer in an Organic Field-effect Transistor. *J. Mater. Chem. C* **2014**, *2*, 4539–4544.
- Xie, T.; Xie, G.; Zhou, Y.; Huang, J.; Wu, M.; Jiang, Y.; Tai, H. Thin Film Transistors Gas Sensors based on Reduced Graphene Oxide Poly(3-hexylthiophene) Bilayer Film for Nitrogen Dioxide Detection. *Chem. Phys. Lett.* **2014**, *614*, 275–281.
- Jaiswal, M.; Menon, R. Polymer Electronic Materials: a Review of Charge Transport. *Polym. Int.* **2006**, *55*, 1371–1384.
- Chung, D. S.; Lee, J. S.; Huang, J.; Nag, A.; Ithurria, S.; Talapin, D. V. Low Voltage Hysteresis Free and High Mobility Transistor from All-inorganic Colloidal Nanocrystals. *Nano Lett.* **2012**, *12*, 1813–1820.
- Kang, I.; Yun, H.-J.; Chung, D. S.; Kwon, S.-K.; Kim, Y.-H. Record High Hole Mobility in Polymer Semiconductors via Side-Chain Engineering. *J. Am. Chem. Soc.* **2013**, *135*, 14896.

(16) Yun, H.-J.; Cho, J.; Chung, D. S.; Kim, Y.-H.; Kwon, S.-K. Comparative Studies on the Relations between Composition Ratio and Charge Transport of Diketopyrrolopyrrole-based Random Copolymers. *Macromolecules*. **2014**, *47*, 7030–7035.

(17) Tseng, H.-R.; Phan, H.; Luo, C.; Wang, M.; Perez, L. A.; Patel, S. N.; Ying, Lei.; Kramer, E. J.; Nguyen, T.-Q.; Bazan, G. C.; Heeger, A. J. High-Mobility Field-Effect Transistors Fabricated with Macroscopic Aligned Semiconducting Polymers. *Adv. Mater.* **2014**, *26*, 2993–2998.

(18) Kim, G.; Kang, S.-J.; Dutta, G. K.; Han, Y.-K.; Shin, T. J.; Noh, Y.-Y.; Yang, C. A Thienoisindigo-Naphthalene Polymer with Ultrahigh Mobility of 14.4 cm²/V·s That Substantially Exceeds Benchmark Values for Amorphous Silicon Semiconductors. *J. Am. Chem. Soc.* **2014**, *136*, 9477–9483.

(19) Sirringhaus, H. 25th Anniversary Article: Organic Field-Effect Transistors: The Path Beyond Amorphous Silicon. *Adv. Mater.* **2014**, *26*, 1319–1335.

(20) Wu, P.-T.; Kim, F. S.; Jenekhe, S. A. New Poly(arylene vinylene)s Based on Diketopyrrolopyrrole for Ambipolar Transistors. *Chem. Mater.* **2011**, *23*, 4618–4624.

(21) Dreyer, D. R.; Park, S.; Bielawski, C. W.; Ruoff, R. S. The Chemistry of Graphene Oxide. *Chem. Soc. Rev.* **2010**, *39*, 228–240.

(22) Rivnay, J.; Mannsfeld, S. C. B.; Miller, C. E.; Salleo, A.; Toney, M. F. Quantitative Determination of Organic Semiconductor Microstructure from the Molecular to Device Scale. *Chem. Rev.* **2012**, *112*, 5488–5519.

(23) Si, P.; Mortensen, J.; Komolov, A.; Denborg, J.; Møller, P. J. Polymer Coated Quartz Crystal Microbalance Sensors for Detection of Volatile Organic Compounds in Gas Mixtures. *Anal. Chim. Acta* **2007**, *597*, 223–230.

(24) Podzorov, V.; Menard, E.; Borissov, A.; Kiryukhin, V.; Rogers, J. A.; Gershenson, M. E. Intrinsic Charge Transport on the Surface of Organic Semiconductors. *Phys. Rev. Lett.* **2004**, *93*, 086602.

(25) Podzorov, V.; Menard, E.; Rogers, J. A.; Gershenson, M. E. Hall Effect in the Accumulation Layers on the Surface of Organic Semiconductors. *Phys. Rev. Lett.* **2005**, *95*, 226601.